

Hot B violation, the lattice, and hard thermal loops

Peter Arnold

Department of Physics, University of Washington, Seattle, Washington 98195

(January 1997)

Abstract

It has recently been argued that the rate per unit volume of baryon number violation (topological transitions) in the hot, symmetric phase of electroweak theory is of the form $\eta \alpha_w^5 T^4$ in the weak-coupling limit, where η is a non-perturbative numerical coefficient. Over the past several years, there have been attempts to extract the rate of baryon number violation from real-time simulations of classical thermal field theory on a spatial lattice. Unfortunately, the coefficient η will not be the same for classical lattice theories and the real quantum theory. However, by analyzing the appropriate effective theory on the lattice using the method of hard thermal loops, I show that the *only* obstruction to precisely relating the rates in the real and lattice theories is the fact that the long-distance physics on the lattice is not rotationally invariant. (This is unlike Euclidean-time measurements, where rotational invariance is always recovered in the continuum limit.) I then propose how this violation of rotational invariance can be eliminated—and the real B violation rate measured—by choosing an appropriate lattice Hamiltonian. I also propose a rough measure of the systematic error to be expected from using simpler, unimproved Hamiltonians. As a byproduct of my investigation, the plasma frequency and Debye mass are computed for classical thermal field theory on the lattice.

I. INTRODUCTION

The violation of baryon number (B) in the hot, symmetric phase¹ of electroweak theory plays a crucial role in scenarios for electroweak baryogenesis. The rate of B violation is tied, through the electroweak anomaly, to the the rate of topological transitions of the electroweak gauge fields. For the symmetric phase, this rate is not calculable by any perturbative method. In this paper, I address whether the topological transition rate can, in principle, be extracted from lattice simulations. The discussion will reveal some surprising features of real-time thermal field theory on the lattice.

It has long been appreciated that, at finite temperature, topological transitions in real time are not directly related to topological transitions in Euclidean time [2]. As a result, there is no apparent way to measure the real-time thermal transition rate in a standard, Euclidean-time, lattice simulation of quantum field theory. Several years ago, Ambjørn and Krasnitz [4] cleverly implemented the observation [5] that a full simulation of *quantum* field theory is not actually required. Topological transitions occur in the symmetric phase through large configurations which are essentially classical. Indeed, *all* long-distance bosonic physics in a hot, ultrarelativistic plasma is effectively classical because of Bose enhancement. The number of quanta per mode in low-energy modes is given by the Bose distribution

$$n(E) \equiv \frac{1}{e^{\beta E} - 1} \sim \frac{1}{\beta E} \gg 1 \quad \text{for} \quad E \ll T, \quad (1.1)$$

and, by the correspondence principle, this is the classical regime. Unlike quantum field theory, real-time simulations of classical field theory are tractable: just evolve the classical equations of motion.

Classical thermal field theory has an ultraviolet catastrophe, historically famous in the context of black-body radiation. Because every mode has energy $\frac{1}{2}T$ by the classical equipar-

¹ Here and throughout, I use the term “symmetric phase” loosely since, depending on the details of the Higgs sector, there may not be any sharp transition between the symmetric and “symmetry-broken” phases of the theory [1,3]. A sharp transition is in fact required for electroweak baryogenesis.

tition theorem, and because there are an infinite number of modes per unit volume in continuum field theory, the energy density is infinite. In quantum field theory, in contrast, the ultraviolet contribution is cut off at momenta of order T . Ambjørn and Krasnitz reasoned that the details of short-distance physics should not affect the long-distance physics of topological transitions. In their simulations, they put their classical system on a spatial lattice and then evolved it in continuous real time. The ultraviolet catastrophe was cut off by the lattice spacing, which they progressively made smaller and smaller.

Son, Yaffe, and I [6] have recently pointed out that short-distance effects do not decouple as cleanly as Ambjørn and Krasnitz hoped. In particular, the short-distance modes cause damping of the long-distance dynamics, and this damping affects the transition rate. We showed that damping reduces the transition rate by a factor of $O(\alpha)$, where α is the weak fine structure constant. Because the damping is caused by short-distance physics, it is not universal, and so a comparison of theories with different short-distance physics becomes non-trivial. In the classical lattice theory used by Ambjørn and Krasnitz, for example, damping reduces the rate instead by a factor of $O(\alpha a T)$ where a is the lattice spacing. As I shall discuss, there is an even more serious problem: because damping is dominated by short-distance physics, it knows about the anisotropies of the lattice. As we shall see explicitly, and as was first noted by Bodeker *et al.* [7], the effective long-distance physics of the classical lattice theory is not even rotationally invariant. This is in striking contrast to the familiar situation of Euclidean-time simulations, where rotational invariance is always recovered in the continuum limit.

I shall assume that our analysis of damping in ref. [6] is correct and will eventually be borne out by numerical simulations at sufficiently weak coupling. In this paper, I focus on the natural follow-up question: Given that the real quantum theory and the classical lattice theory have different long-distance physics, is there any way to measure the real topological transition rate? The answer is yes—in principle—but an exact calculation requires a careful

choice of lattice action and the numerical extraction of a somewhat awkward limit.² But I shall also propose a rough numerical measure of the suitability of generic lattice actions and argue that even results from simple, canonical actions should be in the right ballpark if properly interpreted.

I shall not address at all the complicated problem of how one measures topological transitions on the lattice in the first place, which has a long, difficult history for Euclidean-time quantum simulations³ and a shorter but still confusing one for real-time classical simulations [4,6,11,12]. I simply focus on dynamics and assume the measurement problem will eventually be solved, using cooling or some other technique.

Section 2 of this paper outlines my method for taking a measurement of the topological transition rate in a theory with one ultraviolet cut-off (*e.g.* a classical spatial lattice theory) and using it to predict the rate in the same theory with a different ultraviolet cut-off (*e.g.* the real, continuum, quantum field theory). The procedure will require, however, that the long-distance dynamics be rotationally invariant in both cases, and this poses a problem for the lattice that will eventually be dealt with. Section 2 rests on a very rough and schematic discussion of the effective long-distance dynamics, and I return in section 3 to do a better job of reviewing the correct long-distance theory. I review the derivation of “hard thermal loop” effective theory but add a small twist. The usual discussions in the literature are based on the assumption that hard (*i.e.* high-momentum) excitations in the plasma move at the speed of light. This is not true for lattice theories, and I show how the usual results easily generalize. In section 4, as a warm-up example of a rotational-invariant classical theory, I consider continuum classical thermal field theory with the ultraviolet regulated by higher-derivative interactions. In section 5, I turn to the canonical definition of the classical theory on a simple cubic spatial lattice. By explicit computation, the damping at long distances

² I shall briefly comment on the very different proposal of Hu and Müller [8] in my conclusion.

³ For a brief review, see sec. III.C.1 of ref. [9]. See also table I of ref. [10].

is shown to be anisotropic and to have an interesting structure of cusp and logarithmic singularities in its angular distribution. I discuss the origin of these singularities. Then I argue that measurements of the topological transition rate in simple lattice theories can still (if properly interpreted) be used to estimate the real transition rate, and I propose a rough measure of the systematic error arising from the anisotropy of the lattice. In section 6, I propose that the real transition rate could in principle be measured arbitrarily well from lattice simulations by implementing a lattice version of the higher-derivative continuum theory discussed in section 4. In section 7, I briefly discuss some possibilities of alternative lattice theories that may be more rotational-invariant than the canonical one, yet easier to implement than my proposal of section 6. Section 8 explores two quantities important to thermal field theory but slightly tangential to the main thrust of this paper: the plasma frequency and the Debye mass. I compute both for classical, thermal gauge theory on the lattice. The results provide one test of whether lattice simulations of a given size are indeed in the small coupling limit, and I comment on the application of this test to the simulations of ref. [4]. Section 9 offers my conclusions and a summary of what remains to be done.

II. THE BASICS

The origin of the basic scales associated with topological transitions is reviewed in the introduction of ref. [6], and I shall simply quote here the standard result: topological transitions proceed through non-perturbative gauge configurations of spatial size $R \sim 1/g^2T$. In ref. [6], we then showed that the time scale associated with such transitions is $t \sim 1/g^4T$ and that the transition occurs through slowly varying magnetic configurations.⁴ (More technically, the relevant, low-frequency gauge fields are transversally rather than longitudinally polarized.) My current endeavor can be summarized as follows. Consider the effective long-distance and long-time theory corresponding to frequencies and spatial momenta of order

⁴ See also ref. [13].

$(\omega, k) \sim (g^4 T, g^2 T)$. What is the correspondence of those theories between (a) the real quantum theory, and (b) a cut-off classical theory?

The important characteristics of the long-distance effective theory for topological transitions, as discussed in refs. [6,13], can be roughly introduced as follows: The behavior of the long-distance modes is analogous to a pendulum moving in hot molasses, where the molasses represents the short-distance modes, and non-perturbative physics such as the topological transition rate corresponds to large-amplitude fluctuations of the pendulum. A slightly non-linear pendulum is described by an equation of the form

$$(\partial_t^2 + k^2)A + (\text{higher-order in } A) = 0. \quad (2.1)$$

A pendulum in (idealized) hot molasses is described instead by a Langevin equation of the form

$$(\partial_t^2 + \gamma \partial_t + k^2)A + (\text{higher-order in } A) = \xi(t). \quad (2.2)$$

There is a damping term with coefficient γ due to the viscous interaction with the molasses. There is also a random force $\xi(t)$ due to the buffeting of the pendulum by random thermal fluctuations of the molasses. The two are related by the fluctuation-dissipation theorem. Ignoring the non-linearity of the pendulum, the random force in (2.2) must have a white-noise spectrum with normalization $2\gamma T$:

$$\langle \xi(t') \xi(t) \rangle = 2\gamma T \delta(t' - t). \quad (2.3)$$

The frequency response of such a pendulum is

$$A(\omega) = \frac{\xi(\omega)}{-\omega^2 - i\gamma\omega + k^2}, \quad (2.4)$$

with a power spectrum

$$\langle A(\omega')^* A(\omega) \rangle = \frac{2\gamma T \delta(\omega' - \omega)}{|-\omega^2 - i\gamma\omega + k^2|^2} \quad (2.5)$$

which includes small-amplitude, high-frequency fluctuations and larger-amplitude, low-frequency ones. If the pendulum is strongly damped, $\gamma \gg k$, then the characteristic inverse time for the largest amplitude fluctuations is

$$\omega \sim k^2/\gamma \ll k. \quad (2.6)$$

In this case, the ω^2 term is ignorable in (2.4), and the large-amplitude fluctuations of the system can be described by replacing (2.2) with the simpler equation

$$(\gamma\partial_t + k^2)A + (\text{higher-order in } A) = \xi(t). \quad (2.7)$$

In the case of gauge theory, the damping coefficient⁵ γ is determined from the imaginary part of the (retarded) thermal self-energy $\Pi(\omega, \mathbf{k})$. The effective equation of the long-distance modes is, in frequency and momentum space,

$$(-\omega^2 + \Pi(\omega, \mathbf{k}) + k^2)A + (\text{higher-order in } A) = \xi(\omega, \mathbf{k}), \quad (2.8)$$

where $k \equiv |\mathbf{k}|$. The dominant contribution to Π for $\omega, k \ll T$ is well-known [14] and is generated by interactions with short-distance (momenta $\sim T$) degrees of freedom. In the frequency region of interest ($\omega \ll k \ll T$), and for transverse (*i.e.* magnetic) fluctuations, it is given in weak coupling by

$$\Pi(\omega, \mathbf{k}) \approx -i\omega \frac{\pi m_d^2}{4k}, \quad (2.9)$$

where m_d is the (leading order) Debye mass. For the case of pure gauge theory,

$$m_d^2 = \frac{1}{3}C_A g^2 T^2, \quad (2.10)$$

where C_A is the adjoint Casimir and $C_A = N$ for $SU(N)$. So, for each mode \mathbf{k} , the damping coefficient γ of (2.2) is just

$$\gamma = \frac{\pi m_d^2}{4k}. \quad (2.11)$$

⁵ The reader should not confuse the damping coefficient γ with the plasmon damping rate: they refer to different kinematic regimes. γ describes the damping of nearly-static magnetic fields in the plasma, for which $\omega \ll k$ and $\text{Im } \Pi$ is $O(g^2 T^2 \omega/k)$. In this case, $\text{Im } \Pi$ is dominated by hard contributions. The plasmon damping rate, on the other hand, describes the damping of propagating plasma waves, for which $\omega > k$ and $\text{Im } \Pi$ is $O(g^3 T^2)$ [16]. In this case, the dominant contribution to $\text{Im } \Pi$ depends on soft as well as hard physics.

For the spatial momentum scale of topological fluctuations, $k = O(g^2 T)$, (2.6) confirms that $\omega \sim g^4 T \ll k$ and shows that the effective theory can be described by a simplified Langevin equation of the form (2.7).

So far, I have been very schematic. Most significantly, I have blithely ignored all the terms in the above equations labeled “higher order in A .” Since I am ultimately interested in non-perturbative phenomena, I need to do a better job. I will review the full, unadulterated equations of motion of the effective theory in the next section. However, the schematic equations presented so far are adequate to explain the basic idea of how to compare theories with different ultraviolet behavior.

Ignoring the higher-order terms altogether for now, consider two theories with different ultraviolet cut-offs—say, the real quantum theory and some cut-off classical theory. The self-energy Π will be different in the two theories, and so the damping constant γ will be different. The long-distance effective equations of motion are then also superficially different:

$$(\gamma_1 \partial_t + k^2)A = \xi_1(t) \tag{2.12a}$$

vs.

$$(\gamma_2 \partial_t + k^2)A = \xi_2(t). \tag{2.12b}$$

But, as I’ve written them, these two equations are trivially related by a rescaling of time:

$$t_1 \rightarrow \frac{\gamma_1}{\gamma_2} t_2. \tag{2.13}$$

[That this transformation maps $\xi_1 \rightarrow \xi_2$ can be verified from (2.3).] That means that the topological transition rates Γ of the two theories are related by a simple rescaling of time:

$$\Gamma_1 = \frac{\gamma_2}{\gamma_1} \Gamma_2. \tag{2.14}$$

The prescription for measuring the real topological rate is then: (a) to measure it in some UV cut-off classical theory, (b) to perturbatively compute the self-energy and hence the values of γ in both the real theory and the classical theory, and then (c) to convert the measured rate by (2.14).

The fly in the ointment is that generically, in lattice theories, γ is not rotationally invariant but depends on the direction of \mathbf{k} with respect to the axis of the lattice. I shall demonstrate this later by explicit calculation. This means that there is no single rescaling of time that can relate the equations (2.12) for all the long-distance modes of the theories. So there is another step required in the prescription: (step 0) find a classical lattice theory where the ultraviolet cut-off is as rotationally invariant as possible. I should emphasize that, unlike the more familiar case of Euclidean-time simulations, this last step is a theoretical necessity and not merely a numerical convenience. In Euclidean simulations, improving the rotational invariance of the action improves the rate of approach to the continuum limit as the lattice spacing is decreased, but (in principle) any lattice action will do as long as the lattice spacing is small enough. Here, that is not the case.

The chink in the armor of rotation invariance can already be seen in the result (2.9) for the self-energy in the real, rotational-invariant theory. In Euclidean time, consider effective interactions of the long-distance degrees of freedom that are induced by the short-distance degrees of freedom. Such interactions can be Taylor expanded in the small, long-distance momenta k_x , k_y , and k_z . The cubic symmetry of the lattice is enough to guarantee that any interaction up to two derivatives \mathbf{k} is in fact rotationally invariant as well. Interactions involving four derivatives need not be rotationally invariant, but such interactions are irrelevant and decouple from the long-distance physics. The crucial assumption of this argument is the analyticity of the interactions at $\mathbf{k} = 0$. It has long been known that real-time thermal interactions generated by short-distance physics *fail* this analyticity criterion, as can be seen explicitly in (2.9). The standard mechanism by which rotational invariance is recovered in Euclidean time is therefore no longer operative.

Before proceeding to flesh out the proposals made in this section, I should fix a point of nomenclature. Often in this paper I shall refer to the “real” rate Γ_{real} of topological transitions in continuum, quantum, pure non-Abelian gauge theory at high temperature and weak coupling. If one’s interest is in actual electroweak theory in the same limit, with its accompanying Higgs and fermion fields, it is easy to convert if one ignores the small

effects of the Weinberg mixing angle. The Debye mass in electroweak theory is [15]

$$m_d^2 = \left(\frac{5}{6} + \frac{1}{3}n_f\right) g^2 T^2 \quad (2.15)$$

for a single doublet Higgs and $n_f = 3$ families. By the conversion procedure (2.14) outlined above and by (2.11), the electroweak rate Γ_{ew} is related to the pure SU(2) gauge theory rate “ Γ_{real} ” by

$$\Gamma_{\text{ew}} = \frac{\Gamma_{\text{real}}}{\left(\frac{5}{4} + \frac{1}{2}n_f\right)}. \quad (2.16)$$

Eq. (2.16) and the analysis of this paper applies whenever the temperature is sufficiently high that the infrared dynamics of the Higgs is irrelevant at lengths of $O(1/g^2T)$. This is the case either (1) far above the electroweak phase transition or crossover, or (2) in the symmetric phase at the transition in cases where there is a 1st-order transition and the transition is not exceedingly weak. Other cases could be handled by including the infrared dynamics of the Higgs into the discussion and into simulations.

III. HARD THERMAL LOOPS

A. Review of Basic Derivation

It is now well-established how to write a set of non-local equations describing the dominant interactions of long-distance modes in hot, real-time, non-Abelian gauge theory when the random force term ξ discussed earlier is ignored.⁶ These interactions go by the name of “hard thermal loops,” since they are generated by integrating out the hard, short-distance modes of the theory. Though there is a great deal of literature on this subject, it is almost

⁶ The reader may wonder why numerical simulations don’t simply simulate these equations directly. The problem is their non-locality. For a discussion of the nightmare of trying to find a consistent, local description of the effective theory itself (which requires making precise the separation between soft and hard degrees of freedom), see ref. [7]. I shall be using the hard-thermal-loop equations only as a theoretical tool for comparing the (leading-order) long-distance dynamics of more fundamental, local theories.

universally geared to hard particles that travel at the speed of light. In a lattice theory, in contrast, the hard particles have a more complicated dispersion relationship than $\omega = k$. It will therefore be useful to briefly review the derivation of the hard thermal loop equations so that I can motivate the (simple) modifications required for applying them to lattice theories.

Hard thermal loops were originally derived through diagrammatic analysis by Braaten and Pisarski [16]. For my purpose, the quickest way to get at them is by an alternate method formalized by Blaizot and Iancu [17,18], which I shall present heuristically. (See also ref. [19].) The method is a generalization of the description of QED plasmas via Vlasov equations. The Vlasov equations are an effective description where soft photons are represented by gauge fields $A_\mu(t, \mathbf{x})$ in the usual way, but all the hard, charged particles are represented by a locally defined flow density $n(t, \mathbf{p}, \mathbf{x})$, which is the density of particles at time t and position \mathbf{x} with (hard) momentum \mathbf{p} . The first Vlasov eq. follows from applying Liouville's Theorem to n and using the equations of motion:⁷

$$0 = \frac{d}{dt} n(t, \mathbf{p}, \mathbf{x}) = \partial_t n + \dot{\mathbf{x}} \cdot \partial_{\mathbf{x}} n + \dot{\mathbf{p}} \cdot \partial_{\mathbf{p}} n = v^\mu \partial_\mu n + e(\mathbf{E} + \mathbf{v} \times \mathbf{B}) \cdot \partial_{\mathbf{p}} n, \quad (3.1)$$

where \mathbf{v} is the 3-velocity and where $v^\mu \equiv (1, \mathbf{v})$. (Note that v^μ does not transform as a Lorentz 4-vector.) In the real world of ultrarelativistic plasmas, hard excitations move at the speed of light and \mathbf{v} is just $\hat{\mathbf{p}} = \mathbf{p}/|\mathbf{p}|$. Here enters my simple generalization of the standard discussion in the literature: for more general underlying field theories, \mathbf{v} should be identified with the *group* velocity of the hard excitations, since it is the group velocity which describes the physical rate of motion of charge. If the dispersion relationship for the hard modes is $E = \Omega_{\mathbf{p}}$, then the group velocity is

$$\mathbf{v} = \nabla_{\mathbf{p}} \Omega_{\mathbf{p}}. \quad (3.2)$$

(For those who find this style of argument overly heuristic, an explicit check of final results will be made in Appendix A using a diagrammatic approach.)

⁷ For a discussion of why hard collision terms (*i.e.* terms non-linear in n) can be ignored in the application to topological transitions, see ref. [13].

The second Vlasov equation, which is for the gauge field, is simply

$$\partial_\mu F^{\mu\nu} = j^\nu = \sum_f e_f \int_{\mathbf{p}} v^\nu n_f, \quad (3.3)$$

where I have added a flavor index f to make explicit that there may be different types of particles with different charges in the plasma. I have also introduced the short-hand notation

$$\int_{\mathbf{p}} \equiv \int \frac{d^3p}{(2\pi)^3}. \quad (3.4)$$

Now linearize the Vlasov equations in the gauge fields and in deviations δn of n from its equilibrium distribution n_0 . n_0 depends only on the energy $\Omega_{\mathbf{p}}$ of excitations and not on \mathbf{x} or t . Using

$$\partial_{\mathbf{p}} n_0 = \frac{dn_0}{d\Omega} \partial_{\mathbf{p}} \Omega = \frac{dn_0}{d\Omega} \mathbf{v}, \quad (3.5)$$

the linearized Vlasov equations are

$$v \cdot \partial \delta n_f + e_f \mathbf{E} \cdot \mathbf{v} \frac{dn_0}{d\Omega} = 0, \quad (3.6a)$$

$$\partial_\mu F^{\mu\nu} = \sum_f e_f \int_{\mathbf{p}} v^\nu \delta n_f. \quad (3.6b)$$

These equations can be solved formally for δn , yielding

$$\partial_\mu F^{\mu\nu}(t, \mathbf{x}) = - \sum_f e_f^2 \int_{\mathbf{p}} \frac{dn_0}{d\Omega} \frac{v^\nu v^j}{(v \cdot \partial + \epsilon)} E^j(t, \mathbf{x}). \quad (3.7)$$

ϵ is an infinitesimal that has been inserted to pick out the retarded solutions to the equations.

For QED with a single massless fermion,

$$\partial_\mu F^{\mu\nu} = -4e^2 \int_{\mathbf{p}} \frac{dn_0}{d\Omega} \frac{v^\nu v^j}{(v \cdot \partial + \epsilon)} E^j, \quad (3.8)$$

where the factor of 4 counts the two polarizations each of the fermion and anti-fermion.

It is easy to guess how the forgoing generalizes to non-Abelian gauge theories. From (3.6b) it is clear that the δn of interest must carry an adjoint color index. (Rather than a simple color-diagonal number operator, δn now represents a correlation between the colors that the gauge bosons convert between.) But then the convective derivative $v \cdot \partial$ in (3.6a)

must be generalized to a covariant convective derivative $v \cdot D$, where D is understood to act in the adjoint representation. Similarly, the derivative in (3.6b) should be covariant. The resulting equation for the soft modes is

$$D_\mu F^{\mu\nu} = -2C_A g^2 \int_{\mathbf{p}} \frac{dn_0}{d\Omega} \frac{v^\nu v^j}{(v \cdot D + \epsilon)} E^j, \quad (3.9)$$

where e^2 has been replaced by $C_A g^2$ and the factor of 2 counts the two helicity states of the hard gauge bosons. Readers desiring a much more detailed justification should refer to ref. [18].

For our current application to topological transitions, where frequencies are small compared to spatial momenta and the fluctuations are magnetic, we are only interested in the small frequency limit of (3.9). Working in $A_0 = 0$ gauge, this limit gives

$$(\mathbf{D} \times \mathbf{B})^i = 2C_A g^2 \int_{\mathbf{p}} \frac{dn_0}{d\Omega} \frac{v^i v^j}{(\mathbf{v} \cdot \mathbf{D} + \epsilon)} \partial_t A^j. \quad (3.10)$$

where $\mathbf{B} = \mathbf{D} \times \mathbf{A}$. As long as the energy $\Omega_{\mathbf{p}}$ respects parity, the integral over \mathbf{p} would vanish if not for the ϵ factor. Using

$$\frac{1}{\mathbf{v} \cdot \mathbf{D} + \epsilon} = P \frac{1}{\mathbf{v} \cdot \mathbf{D}} + \pi \delta(\mathbf{v} \cdot i\mathbf{D}), \quad (3.11)$$

where P stands for principal part, the effective equation for the frequencies and momenta of interest may be rewritten as

$$\gamma^{ij}(i\mathbf{D}) \partial_t A^j + (\mathbf{D} \times \mathbf{B})^i = 0, \quad (3.12)$$

where

$$\gamma^{ij}(\mathbf{k}) \equiv -2\pi C_A g^2 \int_{\mathbf{p}} \frac{dn_0}{d\Omega} v^i v^j \delta(\mathbf{v} \cdot \mathbf{k}). \quad (3.13)$$

This is indeed of the form of the “non-linear system in molasses” (2.2) discussed schematically in section II, except that it is missing the random force term.

The underlying diagrammatic origin of the result (3.13) for the damping factor can be roughly understood by considering the process of fig. 1, which shows a soft excitation being

absorbed by the small-angle scattering of a hard excitation. The factor $g v^i$ in (3.13) comes from the interaction vertex, and the second factor $g v^j$ is because the amplitude of fig. 1 should be squared to get a rate. The $\delta(\mathbf{v} \cdot \mathbf{k})$ is just the $\omega \ll k \ll p$ limit of the energy-conserving delta function $\delta(\Omega_{\mathbf{p}+\mathbf{k}} - \Omega_{\mathbf{p}} - \omega)$ associated with this diagram. Finally, $dn/d\Omega$ for a Bose or Fermi distribution is just $-\beta$ times the product $n_0(1 \pm n_0)$ of the initial-state probability distribution and the final-state Bose enhancement or Fermi blocking factor. More details are given in Appendix A.

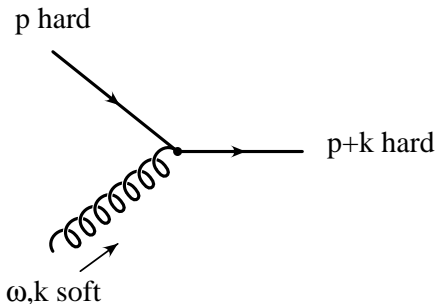


FIG. 1. The absorption of a soft excitation (wavy line) by the small-angle scattering of a hard excitation (straight line).

B. The random force term

The final result (3.12) of the previous section is in fact sufficient for the comparison of different theories, but, for the sake of completeness, I will review the random force term as well. The Vlasov equations of the previous section describe the relaxation or propagation of deviations from equilibrium; they do not, as formulated above, describe the fluctuations that occur in equilibrium itself. However, fluctuations are related to dissipation through the fluctuation-dissipation theorem. Introduce a random force term by writing

$$\gamma^{ij}(i\mathbf{D}) \partial_t A^j + (\mathbf{D} \times \mathbf{B})^i = \xi^i. \quad (3.14)$$

If we momentarily ignore the non-linearity of (3.14), which arises from the non-Abelian nature of the theory, then the characteristics of the random force can be taken from (2.3):

$$\langle \xi^{ia}(t, \mathbf{x}) \xi^{jb}(t', \mathbf{x}') \rangle = 2 \delta^{ab} \gamma^{ij}(i\partial_{\mathbf{x}}) T \delta^{(3)}(\mathbf{x} - \mathbf{x}') \delta(t - t'), \quad (3.15)$$

where a and b are adjoint color indices. Huet and Son [13] have shown how to modify this equation to include the non-linearity and restore gauge invariance. The result is to simply replace δ^{ab} above by a straight, adjoint-charge Wilson line connecting \mathbf{x} to \mathbf{x}' :

$$\langle \xi^{ia}(t, \mathbf{x}) \xi^{jb}(t', \mathbf{x}') \rangle = 2 U^{ab}(t; \mathbf{x}, \mathbf{x}') \gamma^{ij}(\partial_{\mathbf{x}}) T \delta^{(3)}(\mathbf{x} - \mathbf{x}') \delta(t - t'), \quad (3.16)$$

where

$$U(t; \mathbf{x}, \mathbf{x}') = \mathcal{P} \exp \left(- \int_{\mathbf{x}}^{\mathbf{x}'} d\mathbf{z} \cdot \mathbf{A}^a(t, \mathbf{z}) \mathcal{T}^a \right), \quad (3.17)$$

\mathbf{z} runs on a straight path from \mathbf{x} to \mathbf{x}' , \mathcal{P} denotes path ordering, and the \mathcal{T}^a are the (real, anti-Hermitian) adjoint representation generators. The basic equations for the effective theory are then (3.14) and (3.16).

C. Application to rotational-invariant theories

The damping coefficient γ of (3.13) can be rewritten as

$$\gamma^{ij}(\mathbf{k}) = \frac{\pi M^{ij}(\hat{\mathbf{k}})}{4|\mathbf{k}|}, \quad (3.18)$$

where

$$M^{ij}(\hat{\mathbf{k}}) \equiv -8C_A g^2 \int_{\mathbf{p}} \frac{dn_0}{d\Omega} v^i v^j \delta(\mathbf{v} \cdot \hat{\mathbf{k}}) \quad (3.19)$$

depends only on the direction $\hat{\mathbf{k}}$. Note that M is transverse:

$$\hat{k}^i M^{ij}(\hat{\mathbf{k}}) = 0. \quad (3.20)$$

In a theory that is fundamentally rotationally invariant, it must then have the form

$$M^{ij}(\hat{k}) = (\delta^{ij} - \hat{k}^i \hat{k}^j) m^2, \quad (3.21)$$

where m^2 is a number independent of \mathbf{k} , obtained by averaging $\text{tr}M$ over $\hat{\mathbf{k}}$:⁸

⁸ I am using a notation and normalization here that makes m the analog of the m_d in (2.9). However, m is not actually the Debye mass in theories where $|\mathbf{v}| \neq 1$. See section VIII.

$$m^2 = -2C_A g^2 \int_{\mathbf{p}} \frac{dn_0}{d\Omega} |\mathbf{v}|. \quad (3.22)$$

By examining the effective equations (3.14) and (3.16), it is then easy to check that the time rescaling suggested in section II will indeed relate any two rotational-invariant theories:

$$t_1 = \frac{m_1^2}{m_2^2} t_2, \quad \Gamma_1 = \frac{m_2^2}{m_1^2} \Gamma_2. \quad (3.23)$$

If $\Omega_{\mathbf{p}}$ is monotonically increasing, m^2 can be rewritten in the simpler form

$$m^2 = \frac{2C_A g^2}{\pi^2} \int_0^\infty dp p n_0(\Omega_p). \quad (3.24)$$

The result (2.10) for the real quantum theory can now be reproduced by using the massless Bose distribution $(e^{\beta p} - 1)^{-1}$ for $n_0(\Omega_p)$.

IV. AN EXAMPLE: CONTINUUM THEORY WITH HIGHER DERIVATIVES

Before I move on to lattice theories and the difficulties with rotational invariance, it is useful to first make the preceding discussion concrete with a simple, rotational-invariant example of a classical thermal field theory. Consider a classical continuum description of non-Abelian gauge theory where I regulate the ultraviolet by higher-derivative terms.⁹ The Hamiltonian density is

$$H = \text{tr} \left[E^i E^i + B^i f \left(\frac{\mathbf{D}^2}{\Lambda^2} \right) B^i \right], \quad (4.1)$$

where f has an expansion

$$f(z) = 1 + a_1 z + a_2 z^2 + \dots \quad (4.2)$$

⁹ The term “higher derivative theory” often refers to Lorentz-invariant theories, where the action must contain higher time derivatives as well as higher spatial ones. Such theories create annoying issues about initial conditions and negative-norm states. The theory here, however, does not involve higher time derivatives and is free from such complications.

and $\mathbf{E} = -\partial_t \mathbf{A}$ is (minus) the conjugate momentum to \mathbf{A} . At momenta low compared to Λ , this is just normal gauge theory. However, provided $f(z)$ grows sufficiently rapidly at large z , the higher-derivative interactions will cut off the ultraviolet catastrophe of classical thermal field theory at a momentum scale of order Λ .

To compare this cut-off classical theory to the real quantum theory, I will compute the damping coefficient m^2 of (3.24). For any classical theory, the equilibrium distribution $n_0(\Omega)$ is simply

$$n_0(\Omega) = \frac{T}{\Omega}. \quad (4.3)$$

One quick way to see this is to start with the Bose distribution of the quantum theory and, for the first and last time in this paper, put in the explicit factor of \hbar :

$$n_0(\Omega) = \frac{1}{e^{\hbar\beta\Omega} - 1} \rightarrow \frac{T}{\hbar\Omega} \quad \text{as} \quad \hbar \rightarrow 0. \quad (4.4)$$

This just recapitulates the discussion (1.1) of the introduction. The remaining element we need is the frequency $\Omega_{\mathbf{p}}$ as a function of momentum \mathbf{p} for perturbative excitations. For the theory (4.1), it is

$$\Omega_p^2 = p^2 f\left(\frac{p^2}{\Lambda^2}\right). \quad (4.5)$$

The coefficient m^2 of (3.24) is then (for monotonically increasing f)

$$m^2 = \frac{2C_A g^2 T \Lambda}{\pi^2} \int_0^\infty \frac{ds}{\sqrt{f(s^2)}}. \quad (4.6)$$

This converges provided $f(z)$ grows faster than z for large z . In other words, a four-derivative interaction is not enough to cut off the ultraviolet, but six derivatives do the job. By (3.23) and (2.10), the topological transition rate $\Gamma_{\text{h.d.}}$ in this classical, higher-derivative theory is related (in weak coupling) to the rate Γ_{real} in the real (pure gauge) quantum theory by

$$\Gamma_{\text{real}} = \Gamma_{\text{h.d.}} \frac{6\Lambda}{\pi^2 T} \int_0^\infty \frac{ds}{\sqrt{f(s^2)}}. \quad (4.7)$$

It will be useful later on to have the specific result for f of the form $f(z) = 1 + az^2$, corresponding to an isolated six-derivative cut-off. In this case,

$$\Gamma_{\text{real}} = \Gamma_{\text{h.d.}} \frac{3 \Gamma^2\left(\frac{1}{4}\right) \Lambda}{2 \pi^{5/2} a^{1/4} T}, \quad (4.8)$$

where $\Gamma(z)$ is the usual Euler Gamma function.

V. A SIMPLE CUBIC SPATIAL LATTICE

A. Results for γ^{ij}

We now have almost everything we need to compute the damping coefficient γ^{ij} , or equivalently M^{ij} , for lattice theories; we just need the dispersion relationship $\Omega_{\mathbf{p}}$. Let's start by studying the simple, classical, Kogut-Susskind Hamiltonian used by Ambørn and Krasnitz [4] for simulations on a simple cubic (SC), spatial lattice. The tree-level dispersion relationship for propagating excitations on the lattice is

$$\Omega_{\mathbf{p}}^2 = 4a^{-2} \left[\sin^2\left(\frac{p_x a}{2}\right) + \sin^2\left(\frac{p_y a}{2}\right) + \sin^2\left(\frac{p_z a}{2}\right) \right], \quad (5.1)$$

where a is the lattice spacing. For thermal field theory on the lattice, the parameters g^2 , a , and T always appear in the combination $g^2 a T$ for dimensionless quantities.¹⁰ I shall henceforth work in lattice units by setting $a = T = 1$. The conversion back to physical ones¹¹ is $g_{\text{lat}} \rightarrow g^2 a T$, $p_{\text{lat}} \rightarrow a p$, $\omega_{\text{lat}} \rightarrow a \omega$, and $t_{\text{lat}} \rightarrow a^{-1} t$.

The group velocity $\nabla \Omega$ is

$$v^i = \frac{\sin p^i}{\Omega_{\mathbf{p}}}. \quad (5.2)$$

Plugging into (3.13) with the classical distribution (4.3) then yields¹²

¹⁰ This is because g^2 and a can be scaled out of the Hamiltonian H so that the distribution $\exp(-\beta H)$ becomes $\exp(-H/g^2 a T)$.

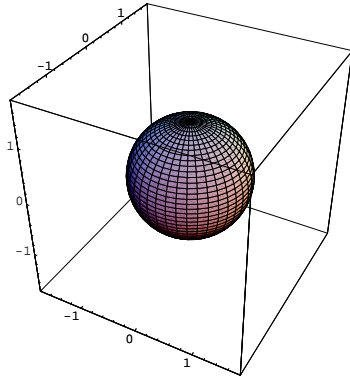
¹¹ Lattice papers such as [4] typically refer to the quantity $\beta_L \equiv 2N/g_{\text{lat}}^2$ for $\text{SU}(N)$ rather than g_{lat}^2 .

¹² A general formula for the hard contribution to Π^{ij} in a simple cubic lattice theory was first written down for QED coupled to massless scalars in eq. (B11) of ref. [7]. My (5.3) is that equation's $\omega \ll k$ limit, once the overall normalization in ref. [7] is changed to be appropriate for pure, non-Abelian gauge theory.

$$\gamma^{ij}(\mathbf{k}) = \frac{\pi M^{ij}(\hat{\mathbf{k}})}{4|\mathbf{k}|}, \quad (5.3a)$$

$$M^{ij}(\hat{\mathbf{k}}) = 8C_A g^2 \int_{-\pi}^{+\pi} \frac{d^3 p}{(2\pi)^3} \frac{\sin p_i \sin p_j}{\Omega_{\mathbf{p}}^3} \delta(\hat{\mathbf{k}} \cdot \sin \mathbf{p}), \quad (5.3b)$$

where the integrals are over the Brillouin zone $|p_i| \leq \pi$.



(a)

(b)

(c)

FIG. 2. The trace γ^{ii} of the damping coefficient as a function of direction, normalized by its angular average, for (a) a rotationally invariant theory, (b) a Kogut-Susskind Hamiltonian on a simple cubic lattice, and (c) for a face-centered cubic lattice. The spikes in (b) and (c) represent logarithmic divergences.

The delta function can be used to eliminate one of the three integrations, and I have done the remaining two numerically. (The detailed expression is given in Appendix B.) Fig. 2b shows the resulting angular distribution of the trace γ^{ii} normalized by its angular average $\langle \gamma^{ii} \rangle$. Not only is the result not rotationally invariant, but it has an interesting structure of singularities as well. There are cusps and, in certain special directions, γ^{ij} is infinite! As we shall see, these singularities are mild and integrable. Also, they are true singularities only in the weak-coupling limit: they are rounded off by higher-order corrections but become sharper and sharper as $g \rightarrow 0$.

B. The origin of singularities

For any fixed direction $\hat{\mathbf{k}}$ of the soft momentum, γ^{ij} as given by (3.13) can be rewritten

$$\gamma^{ij}(\mathbf{k}) \equiv -2\pi C_A g^2 \int_S \frac{dn_0}{d\Omega} \frac{v^i v^j}{|\nabla_{\mathbf{p}}(\mathbf{v} \cdot \mathbf{k})|}, \quad (5.4)$$

where the integral is over the surface S in \mathbf{p} space on which $\mathbf{v}(\mathbf{p})$ is orthogonal to \mathbf{k} . If there is a point on this surface where the vector $\nabla_{\mathbf{p}}(\mathbf{v} \cdot \mathbf{k})$ vanishes, there will be a singularity in γ . If there is an entire line of points where the vector vanishes, the singularity will be more severe. This is analogous to Van Hove singularities in the density of states.¹³ Naive counting of constraints suggests the existence of singularities is to be expected: 5 degrees of freedom in \mathbf{p} and $\hat{\mathbf{k}}$ versus 4 constraints in $\mathbf{v} \cdot \hat{\mathbf{k}} = 0$ and $\nabla_{\mathbf{p}}(\mathbf{v} \cdot \hat{\mathbf{k}}) = 0$.

To summarize, singularities in γ will be caused by momenta \mathbf{p} such that there is a null vector $\hat{\mathbf{k}}$, orthogonal to $\mathbf{v} = \nabla\Omega_{\mathbf{p}}$, of the matrix $\nabla\mathbf{v} = \nabla\nabla\Omega_{\mathbf{p}}$. In the case of the dispersion relationship (5.1),

$$\nabla^i \nabla^j \Omega_{\mathbf{p}} = \frac{\delta^{ij} \cos p^i - v^i v^j}{\Omega_{\mathbf{p}}}. \quad (5.5)$$

At $\mathbf{p} = (\pi/2, \pi/2, \pi/2)$ and its lattice reflections, this matrix is proportional to $v^i v^j$ and so every direction of $\hat{\mathbf{k}}$ orthogonal to $\mathbf{v} \propto (1, 1, 1)$ is associated with a singularity of γ . This is the origin of the cusp singularities in fig. 2b, which are along the plane $k_x + k_y + k_z = 0$ and its three lattice reflections.

For $\mathbf{p} = (\pi/2, \pi/2, p_z)$ and general p_z , the matrix (5.5) has $(1, -1, 0)$ as a null vector, which is orthogonal to v . Therefore, $\hat{\mathbf{k}}$ in the $(1, -1, 0)$ direction or its lattice reflections is associated with an entire line of singularities in \mathbf{p} space. This is the origin of the infinities in these $\hat{\mathbf{k}}$ directions in fig. 2b. (See section VII B for a more general discussion.) For these values of $\hat{\mathbf{k}}$, $\nabla_{\mathbf{p}}(\mathbf{v} \cdot \hat{\mathbf{k}})$ vanishes linearly as one approaches the \mathbf{p} -space line of singularities. The surface integral in (5.4) is therefore only logarithmically singular.

Physically, there are not, in fact, infinite spikes in the angular distribution of $\text{Im} \Pi(\omega, \mathbf{k})$ in the lattice theory. Recall that $(\omega, k) \sim (g^4, g^2)$ for the long-distance physics of interest.

¹³ The density of states is $\rho(E) = \int_p \delta(E - \Omega_{\mathbf{p}})$ and has singularities (typically cusps) when $\mathbf{v} = \nabla\Omega_{\mathbf{p}}$ vanishes for some \mathbf{p} .

The infinite size of the spikes occurs only in the formal limit $\omega \ll k \ll 1$ that I applied to study the theory in weak coupling. The taming of the singularity can be seen from the Vlasov equations by returning to the hard-thermal loop equation (3.9) before extracting the small ω limit. The imaginary part of the self-energy, for spatial polarizations, is

$$\text{Im } \Pi^{ij} = 2C_A g^2 \omega \int_{\mathbf{p}} \frac{dn_0}{d\Omega} v^i v^j \delta(v \cdot K), \quad (5.6)$$

where K is the four-vector (ω, \mathbf{k}) . The relevant difference from the earlier derivation of the damping constant γ^{ij} of (3.13) is simply that $\delta(\mathbf{v} \cdot \mathbf{k})$ has been replaced by $\delta(\mathbf{v} \cdot \mathbf{k} - \omega)$. This difference is sufficient to cut off the logarithmic infinities in γ^{ij} from order $g^2 k^{-1} \ln \infty$ to order $g^2 k^{-1} \ln(k/\omega) \sim g^2 k^{-1} \ln(1/g^2)$.

It is beyond my present purpose to explore the cut off of the logarithmic singularities in detail, but I should mention that the previous paragraph is misleadingly incomplete. Based on the Vlasov equations, I've shown how the logarithms are cut off by effects sub-leading in the limit $\omega \ll k \ll 1$. At sub-leading order, however, the Vlasov equations themselves are inadequate. One can see this from a more fundamental, diagrammatic analysis of the self-energy, discussed in Appendix A. The $\delta(v \cdot K)$ discussed above is nothing more than the $\omega, k \ll p$ limit of the energy-conserving delta function $\delta(\Omega_{\mathbf{p}+\mathbf{k}} - \Omega_{\mathbf{p}} - \omega)$ associated with fig. 1 and discussed at the end of section III A. For (ω, \mathbf{k}) of order (g^4, g^2) in coupling, however, the correct sub-leading version is

$$\delta(\omega_{\mathbf{p}+\mathbf{k}} - \omega_{\mathbf{p}} - \omega) \approx \delta(\mathbf{v} \cdot \mathbf{k} - \omega + \frac{1}{2} \mathbf{k} \cdot \nabla_{\mathbf{v}} \cdot \mathbf{k}). \quad (5.7)$$

The $\mathbf{k} \cdot \nabla_{\mathbf{v}} \cdot \mathbf{k}$ term is the same order as the ω term. Physically, it represents dispersion of the wave packets of the hard excitations—an effect not built into the Vlasov equations' implicit treatment of hard excitations as a collection of classical particles.

In any case, the divergences in the small-coupling limit are only logarithmic and so are mild enough not to cause any real problem with the effective theory specified by (5.3b). Topological transitions occur through configurations with spatial size $1/g^2 T$ and not through pure, infinite-extent, plane waves with momenta \mathbf{k} precisely in one of the divergent directions.

Since logarithmic singularities are integrable in $\hat{\mathbf{k}}$, they will give only a finite damping effect to the evolution of any spatially localized configuration.

C. Estimating the real transition rate

If there were no infinite spikes, fig. 2b would look like at least a rough approximation to the rotational-invariant sphere of fig. 2a, and a procedure for estimating the real, quantum transition rate Γ_{real} suggests itself: replace γ by its appropriate angular average $\bar{\gamma}$, and use this value to relate the lattice measurement of Γ to Γ_{real} as in (2.14) and section III C. What would be the expected systematic error of this procedure? Suppose $\gamma_{\text{max}}(k)$ and $\gamma_{\text{min}}(k)$ were the maximum and the minimum of the angular distribution of $\gamma(\mathbf{k})$. (I shan't worry about the indices i, j on γ^{ij} for the moment.) Since the effect of damping decreases the transition rate, it seems reasonable that the measured Γ is bigger than it would have been if $\gamma(\mathbf{k})$ had been isotropically equal to γ_{max} in all directions but smaller than if $\gamma(\mathbf{k})$ had been isotropically equal to γ_{min} in all directions. So the ratio of the extreme values γ_{min} and γ_{max} to $\bar{\gamma}$ would give a conservative estimate of the relative systematic error due to the anisotropy of the damping.

I shall discuss later whether one might find lattice theories for which $\gamma(\mathbf{k})$ indeed has no infinite spikes. For the moment, focus on the case at hand. Since the spikes are integrable, we can still replace γ by its average to obtain an estimate of Γ_{real} from the lattice measurement of Γ . $\bar{\gamma}$ is the damping felt by isotropic gauge configurations. The problem that remains is to find a plausible estimate of the systematic error, so that there is a measure for deciding whether one lattice theory with spikes is better than another. One obvious candidate is the root-mean-square deviation σ_γ given by $\sigma_\gamma^2 = \overline{(\gamma - \bar{\gamma})^2}$, where the overline indicates angular averaging.

I have suppressed spatial indices on γ above and will now be more concrete. By comparison with the rotational-invariant case, where $\gamma^{ij}(\mathbf{k})$ has the form

$$\gamma^{ij}(\mathbf{k}) = (\delta^{ij} - \hat{k}^i \hat{k}^j) \gamma(k) \tag{5.8}$$

due to its transversality, define

$$\bar{\gamma}^{ij}(\mathbf{k}) \equiv (\delta^{ij} - \hat{k}^i \hat{k}^j) \bar{\gamma}(k), \quad (5.9)$$

$$\bar{\gamma}(k) \equiv \frac{1}{2} \langle \gamma^{ii}(\mathbf{k}) \rangle_{\hat{\mathbf{k}}}, \quad (5.10)$$

for the lattice case, where $\langle \cdots \rangle_{\hat{\mathbf{k}}}$ denotes averaging over the direction of \mathbf{k} . The variation is

$$\sigma^2 \equiv \frac{1}{2} \langle \gamma^{ij}(\mathbf{k}) \gamma^{ij}(\mathbf{k}) \rangle_{\hat{\mathbf{k}}} - [\bar{\gamma}(k)]^2. \quad (5.11)$$

Using the general result (3.13) for γ^{ij} in any theory, we have

$$\bar{\gamma}(k) = -\frac{\pi C_A g^2}{2k} \int_{\mathbf{p}} \frac{dn_0}{d\Omega} |\mathbf{v}| \quad (5.12)$$

and

$$\frac{\sigma^2}{\bar{\gamma}^2} = \frac{\int_{\mathbf{p}} \int_{\mathbf{p}'} \frac{dn_0}{d\Omega} \frac{dn'_0}{d\Omega'} \frac{4(\mathbf{v} \cdot \mathbf{v}')^2}{\pi |\mathbf{v} \times \mathbf{v}'|}}{\left(\int_{\mathbf{p}} \frac{dn_0}{d\Omega} |\mathbf{v}| \right)^2} - 1. \quad (5.13)$$

For the Kogut-Susskind Hamiltonian on a simple cubic lattice, numerical integration gives $\sigma/\bar{\gamma} = 0.31$ and

$$\bar{\gamma}(k) = 0.2687 \frac{C_A g^2}{k}. \quad (5.14)$$

Using (3.23) and (2.11), one can then estimate the real transition rate (in the weak coupling limit) from a lattice measurement as follows. The B violation rate Γ is expected to scale as α^5 in weak coupling [6]. In lattice units, measure the proportionality constant

$$\eta_1 \equiv \lim_{g_{\text{lat}} \rightarrow 0} \frac{\Gamma_{\text{lat}}}{g_{\text{lat}}^{10}}. \quad (5.15)$$

Then the estimate is

$$\Gamma_{\text{real}} \approx \frac{12 \times 0.2687}{\pi} \eta_1 g^{10} T^4. \quad (5.16)$$

The fact that the rough indicator $\sigma/\bar{\gamma}$ of the systematic error due to using the lattice is about 30% suggests that the estimate (5.16) should at least be in the right ballpark of the

true answer. (Also, the minimum value of $\text{tr } \gamma(\hat{\mathbf{k}})$ in fig. 2b is just 30% below the average.) Unfortunately, η_1 has not yet been measured,¹⁴ and even the weak-coupling scaling law $\Gamma \sim \alpha^5$ has yet to be verified on the lattice.

VI. ACHIEVING THE ROTATIONAL-INVARIANT LIMIT

To eliminate the fundamental systematic uncertainty caused by the anisotropy of the lattice, one needs to find an effectively rotational-invariant lattice theory. (I re-emphasize that the search for an alternative theory is a theoretical necessity: just taking the small lattice spacing limit is by itself inadequate.) As it turns out, an effectively rotational-invariant theory is, in principle, easy to achieve. The idea is simply to start with a rotational-invariant continuum theory with a higher derivative cut-off, such as discussed in section IV, and then put it on a lattice that is fine compared to the continuum cut-off scale Λ^{-1} . A numerical extraction of Γ would then require a careful double limit:

$$\lim_{a\Lambda \rightarrow 0} \lim_{g_{\text{lat}} \rightarrow 0} \Gamma_{\text{lat}}, \quad (6.1)$$

where the order of limits is crucial.

To be a little more specific about how the cut-off Λ might be achieved on a spatial lattice, consider the tree-level dispersion relationship for propagating gluons with momentum small compared to the lattice spacing. For a given lattice Hamiltonian (with cubic symmetry), it will have an expansion in momentum of the form

$$s\Omega_{\mathbf{p}}^2 = b|\mathbf{p}|^2 + [c_1|\mathbf{p}|^4 + c_2(p_x^4 + p_y^4 + p_z^4)] + O(p^6) \quad (6.2)$$

in lattice units, where the coefficient s is just a reminder that the units of time can be normalized arbitrarily. By including next-to-nearest-neighbor couplings, and perhaps next-to-next-to-nearest neighbor couplings, and so forth, the parameters of the interactions can be

¹⁴ η_1 should not be confused with the coefficient κ presented in ref. [4], which was an attempt to extract the coefficient of a presumed $\Gamma \sim \alpha^4$ scaling law for weak coupling—a scaling law which ignores the effects of damping [6].

tuned to make any finite set of the coefficients b, c_1, c_2, \dots of the expansion take on whatever values desired. In particular, there is some local Hamiltonian $H_\epsilon^{(4)}$ for which (1) b is a small number, which I'll call ϵ^2 , (2) c_1 is $O(1)$, (3) $c_2 = 0$, and (4) all other coefficients are $\leq O(1)$:

$$s\Omega_{\mathbf{p}}^2 = \epsilon^2 |\mathbf{p}|^2 + c_1 |\mathbf{p}|^4 + O(p^6). \quad (6.3)$$

Choosing units of time where $s = \epsilon^2$,

$$\Omega_{\mathbf{p}}^2 = |\mathbf{p}|^2 + \frac{c_1}{\epsilon^2} |\mathbf{p}|^4 + O\left(\frac{1}{\epsilon^2} p^6\right). \quad (6.4)$$

This describes a theory with a rotational-invariant four-derivative ‘‘cut off’’ at momentum $\Lambda = \epsilon a^{-1}$, plus anisotropic terms that are suppressed by ϵ^2 at that scale.

Unfortunately, the four-derivative ‘‘cut-off’’ in (6.4) is inadequate. As discussed in section IV, a six-derivative interaction is required to cut off the UV contribution to damping. So, even for small ϵ , a generic theory with dispersion relationship (6.3) will still produce significant anisotropy.¹⁵ We can fix the cut-off by going to six derivatives, requiring improved Hamiltonians $H_\epsilon^{(6)}$ where (1) b is a small number, which I'll now call ϵ^4 , (2) the fourth-order coefficients c_1 and c_2 vanish, (3) the coefficient of $|\mathbf{p}|^6$ is $O(1)$, (4) the sixth-order coefficients that break rotational invariance vanish, and (5) other coefficients are $\leq O(1)$:

$$s\Omega_{\mathbf{p}}^2 = \epsilon^4 |\mathbf{p}|^2 + d_1 |\mathbf{p}|^6 + O(p^8), \quad (6.5)$$

Choosing units of time where $s = \epsilon^4$,

$$\Omega_{\mathbf{p}}^2 = |\mathbf{p}|^2 + \frac{d_1}{\epsilon^4} |\mathbf{p}|^6 + O\left(\frac{1}{\epsilon^4} p^8\right). \quad (6.6)$$

This describes the desired rotational-invariant six-derivative cut-off at momentum $\Lambda = \epsilon a^{-1}$ plus anisotropies that are suppressed by ϵ^2 at that scale. The relative size of the anisotropies in the damping coefficient γ will therefore be $O(\epsilon^2)$ and disappear in the limit $\epsilon \rightarrow 0$.

¹⁵ The relative contribution of $\mathbf{p} \sim 1$ to the damping rate is actually $O(1/\ln \epsilon)$ and so, technically, is small in the limit that $\ln \epsilon$ was very large. But this is certainly an impractical limit for any numerical simulation, keeping in mind that, as discussed below, the $\epsilon \rightarrow 0$ and $g_{\text{lat}} \rightarrow 0$ limits do not commute.

I will not attempt in the present work to explicitly construct the improved lattice Hamiltonian $H_\epsilon^{(6)}$ which gives this behavior. A very nice discussion of improving lattice Hamiltonians is given by Moore in ref. [20], where he constructs a classical Yang-Mills Hamiltonian with vanishing p^4 terms. Constructing a Hamiltonian that satisfies the other constraints for $H_\epsilon^{(6)}$ is presumably straightforward in principle but tedious in practice.

In everything above, I have referred to conditions on the tree-level dispersion relationship. The real dispersion relationship for hard excitations ($p \sim \Lambda$) will be modified by perturbative corrections, whose strength is parametrized by $g_{\text{lat}}/\Lambda a = g_{\text{lat}}/\epsilon$. This is the reason that taking the $g_{\text{lat}} \rightarrow 0$ limit before the $\Lambda a \rightarrow 0$ limit would be crucial to extracting results from numerical simulations.

For an improved Hamiltonian giving the desired low-momentum dispersion relation (6.5), the conversion of lattice measurements to the real transition rate would be achieved by first measuring the coefficient

$$\eta_2 \equiv \lim_{\epsilon \rightarrow 0} \lim_{g_{\text{lat}} \rightarrow 0} \frac{\epsilon \Gamma_{\text{lat}}}{g_{\text{lat}}^{10}} \quad (6.7)$$

and then taking

$$\Gamma_{\text{real}} = \frac{3 \Gamma^2\left(\frac{1}{4}\right) \eta_2}{2 \pi^{5/2} d_1^{1/4}} g^{10} T^4, \quad (6.8)$$

which follows from (4.8). g_{lat}^2 above continues to mean $g^2 a T$ where g^2 is the continuum coupling extracted from the Hamiltonian $H_\epsilon^{(6)}$.

VII. OTHER LATTICE THEORIES

A. The FCC lattice

The $a\Lambda \rightarrow 0$ limit discussed in the last section may be difficult to extract numerically. So it's worthwhile to consider whether there are relatively simple lattice theories where the damping coefficient γ , though anisotropic, is closer to rotational invariance than for the simple lattice Hamiltonian discussed in section V. I will briefly discuss here one possibility

for improvement: replacing the simple cubic lattice by a face-centered cubic (FCC) lattice.¹⁶ The FCC lattice can plausibly lead to more rotational-invariant results because sites have more nearest neighbors than for the simple cubic lattice (eight instead of six).

The formulation of lattice QED on a spatial FCC lattice is discussed by Gosar in ref. [23]. The fundamental plaquettes of an FCC lattice are equilateral triangles, and Gosar studies a simple Kogut-Susskind Hamiltonian defined on those plaquettes. All I need here is the dispersion relation, which will be the same for a non-Abelian gauge theory as for photons in QED and is given by Gosar. For a simple cubic lattice, there are three orientations of links (\hat{x} , \hat{y} , and \hat{z}) and three branches of excitations: two, degenerate, propagating polarizations with energy (5.1); and one non-propagating polarization with $\Omega_{\mathbf{p}} = 0$. For an FCC lattice there are six orientations of links and so six branches of excitations [23]:

$$(a) \quad \Omega_{\mathbf{p}}^2 = 0, \quad (7.1)$$

$$(b) \quad \Omega_{\mathbf{p}}^2 = 32, \quad (7.2)$$

$$(c,d) \quad \Omega_{\mathbf{p}}^2 = 32 \left[1 - \sqrt{1 - \epsilon_{\mathbf{p}}/16} \right], \quad (7.3)$$

$$(e,f) \quad \Omega_{\mathbf{p}}^2 = 32 \left[1 + \sqrt{1 - \epsilon_{\mathbf{p}}/16} \right], \quad (7.4)$$

where $\epsilon_{\mathbf{p}}$ is the energy a massless scalar field with nearest-neighbor coupling would have on an FCC lattice,

$$\epsilon_{\mathbf{p}} \equiv 4 \left[3 - \cos \frac{p_x}{2} \cos \frac{p_y}{2} - \cos \frac{p_y}{2} \cos \frac{p_z}{2} - \cos \frac{p_z}{2} \cos \frac{p_x}{2} \right]. \quad (7.5)$$

I have used lattice units where the side of a unit cell is $a = 1$.¹⁷ In the long wavelength limit, branches (c,d) correspond to the two polarizations of the continuum case $\Omega = |\mathbf{p}|$.

¹⁶ In four-dimensional Euclidean gauge theories, people have tried different lattice types for the merely practical reason of trying to speed approach the continuum limit. Lattices used include the F_4 lattice [21], which is the four-dimensional analog of an FCC lattice, and the body-centered hypercubic (BCH) lattice [22].

¹⁷ Ref. [23] instead uses units where the distance between nearest neighbors is 1.

The non-propagating branches (a) and (b) do not contribute to the damping coefficient γ because their group velocity is zero.

The shape of the first Brillouin zone of an FCC lattice is slightly complicated (a “truncated octahedron”), but all that is needed here is that the cube $|p_i| \leq 2\pi$ in momentum space covers the unique momentum states exactly twice. So, when integrating over states, I take

$$\int_{\mathbf{p}} \rightarrow \frac{1}{2} \sum_{\pm} \int_{-2\pi}^{+2\pi} \frac{d^3 p}{(2\pi)^3}. \quad (7.6)$$

The sum is a notational reminder to sum over the two dispersion relationships

$$\Omega_{\mathbf{p}}^2 = 32 \left[1 \pm \sqrt{1 - \epsilon_{\mathbf{p}}/16} \right]. \quad (7.7)$$

The corresponding group velocities are

$$v_x = \pm \frac{\sin \frac{p_x}{2} \left(\cos \frac{p_y}{2} + \cos \frac{p_z}{2} \right)}{\Omega_{\mathbf{p}} \sqrt{1 - \epsilon_{\mathbf{p}}/16}} \quad (7.8)$$

and its permutations.

Numerical evaluation of the general formula (3.13) for γ (see Appendix B) gives the angular distribution of $\text{tr } \gamma$ shown in fig. 2c. The position of the logarithmic spikes is explained in the next section. Numerical integration of (5.12) and (5.13) gives $\bar{\gamma}(k) = 0.501(1) C_A g^2/k$ and $\sigma_{\gamma}/\bar{\gamma} = 0.26(1)$. The 26% result for the angular deviation of damping on the FCC lattice is indeed better than the 31% result for the SC lattice, but not by a lot. The minimum of $\text{tr } \gamma(\hat{\mathbf{k}})$ in fig. 2c is 20% below the average.

B. Avoiding logarithmic spikes

The simplest actions on both the SC and FCC lattices have logarithmic spikes in the angular distribution of γ , shown in figs. 2b and c. In the proposal of section VI for reaching the rotational-invariant limit, it doesn't matter whether the hardest modes $\mathbf{p} \sim 1$ of the theory give rise to such spikes, because the effect of the hardest modes, and hence the strength of

the spikes, will vanish as $\epsilon \rightarrow 0$. For the purposes of surveying simpler lattice theories that are only approximately rotationally invariant, however, it's interesting to consider whether it's possible to avoid the spikes altogether. So I will take a moment to explain the generic property of the simple SC and FCC actions that causes the spikes and then discuss whether it can be avoided.

Recall the conditions $\hat{\mathbf{k}} \cdot \nabla \Omega = 0$ and $\hat{\mathbf{k}} \cdot \nabla \nabla \Omega = 0$ of section V B for generating some sort of singularity. Consider the energy $\Omega_{\mathbf{p}}$ of excitations for small but fixed p_z in a lattice theory with cubic symmetry. Fig. 3a shows a qualitative contour plot of energy $\Omega_{\mathbf{p}}$ vs. p_x and p_y for some such lattice theory [*e.g.* the simple cubic theory of (5.1)]. There is a minimum at $p_x = p_y = 0$, which there must be if we are plotting the branch of $\Omega_{\mathbf{p}}$ that approaches the continuum limit $\Omega_{\mathbf{p}} = |\mathbf{p}|$ for small \mathbf{p} . Suppose that there is also a maximum somewhere along the line $p_x = p_y$, as shown in fig. 3a. Then one can argue as follows that there must be a singularity associated with the direction $\hat{\mathbf{k}} = (1, -1, 0)$ and with \mathbf{p} somewhere on the line $p_x = p_y$ (p_z still fixed). By reflection symmetry through the plane $p_x = p_y$, the group velocity $\nabla \Omega$ on the line must be perpendicular to $\hat{\mathbf{k}}$, and the curvature $\nabla \nabla \Omega$ on the line must have the block-diagonal form

$$\nabla \nabla \Omega = \begin{pmatrix} A & B & 0 \\ B & A & 0 \\ 0 & 0 & C \end{pmatrix}, \quad (7.9)$$

in the basis $(p_z, p_x + p_y, \hat{\mathbf{k}})$. Near the minimum in the fixed p_z plane, C must be negative. Near the maximum that by assumption lies on the line $p_x = p_y$, it must be positive. Therefore, there is a point inbetween where $C = 0$ and so $\hat{\mathbf{k}} \cdot \nabla \nabla \Omega = 0$. This point then satisfies both conditions for generating a singularity associated with the direction $\hat{\mathbf{k}} = (1, -1, 0)$.

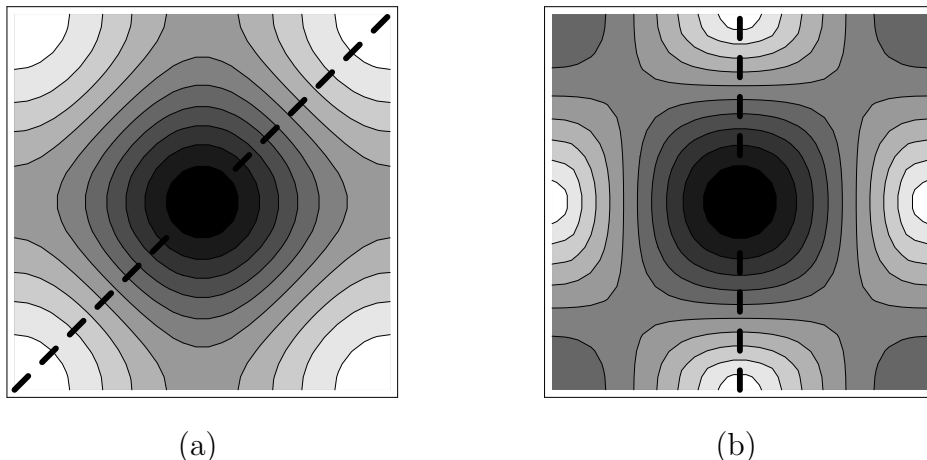


FIG. 3. A qualitative contour plot of $\Omega_{\mathbf{p}}$ vs. p_x and p_y for small, fixed p_z in two different lattice theories. Black corresponds to low values of $\Omega_{\mathbf{p}}$ and white to high ones.

But now note that this argument did not depend on the value of p_z . As long as the assumption that both a minimum and a maximum in (p_x, p_y) simultaneously lie on the line $p_x = p_y$ holds for some *range* of p_z , then there will be an entire curve of points in \mathbf{p} space that contributes to the singularity in the $\hat{\mathbf{k}} = (1, -1, 0)$ direction. As discussed earlier, such degeneracy gives rise to a logarithmic singularity in γ .

A similar qualitative situation, for some different lattice theory [*e.g.* the FCC theory of (7.3)], is shown in fig. 3b. The same argument now goes through with the direction $\hat{\mathbf{k}} = (1, 0, 0)$ and the plane of symmetry $p_x = 0$. This is the origin of the spikes in the FCC case of fig. 2c.

To avoid spikes, look for lattice theories such that $\Omega_{\mathbf{p}}$ does *not* have lines of local maxima and minima in (p_x, p_y) that simultaneously lie on the same plane of symmetry. To show that this is possible, I will give an example from massless scalar QED on a simple cubic lattice (where momenta are $|\mathbf{p}_i| \leq \pi$). For scalar QED, the problem can be reduced to searching through the space of $\Omega_{\mathbf{p}}^2$ that are finite linear combinations of $\sin^2(\mathbf{n} \cdot \mathbf{p}/2)$ for integer vectors \mathbf{n} . This is because one can generate any such $\Omega_{\mathbf{p}}^2$,

$$\Omega_{\mathbf{p}}^2 = \sum_{\mathbf{n}} c_{\mathbf{n}} \sin^2 \left(\frac{\mathbf{n} \cdot \mathbf{p}}{2} \right), \quad (7.10)$$

by a gauged version of the local scalar interaction

$$H_{\text{scalar}} = \sum_{\mathbf{x}} |\Pi_{\mathbf{x}}|^2 + \sum_{\mathbf{x}} \sum_{\mathbf{n}} \frac{c_{\mathbf{n}}}{4} |\phi_{\mathbf{x}} - \phi_{\mathbf{x}+\mathbf{n}}|^2, \quad (7.11)$$

where Π is conjugate to ϕ . So I will therefore first construct an $\Omega_{\mathbf{p}}$ that works and then leave it as an exercise to the interested reader to construct the corresponding Hamiltonian. The space of linear combinations of $\sin^2(\mathbf{n} \cdot \mathbf{p}/2)$ is equivalent, by trigonometric identities, to the space of parity-even polynomials in $\cos p_i$ and $\sin p_i$.

A simple example of an $\Omega_{\mathbf{p}}$ that avoids spikes is

$$[\Omega_{\mathbf{p}}^{(1)}]^2 = 4 - 2 \prod_i (1 + \cos p_i). \quad (7.12)$$

This example is a bit degenerate: the boundary of the Brillouin zone $|\mathbf{p}_i| \leq \pi$ is a constant energy surface, $\Omega_{\mathbf{p}}^2 = 4$. A contour plot of $\Omega_{\mathbf{p}}$ for fixed p_z is shown in fig. 4a. There is a maximum along planes of symmetry, but it is a degenerate maximum. The nominal conditions for a singularity in the damping rate are met but only at the boundary, and at the boundary the group velocity \mathbf{v} corresponding to (7.12) vanishes. The explicit factors of v^i and v^j in the formula (3.13) for γ then compensate the divergence of the $\delta(\mathbf{v} \cdot \mathbf{k})$, and there are no singularities.

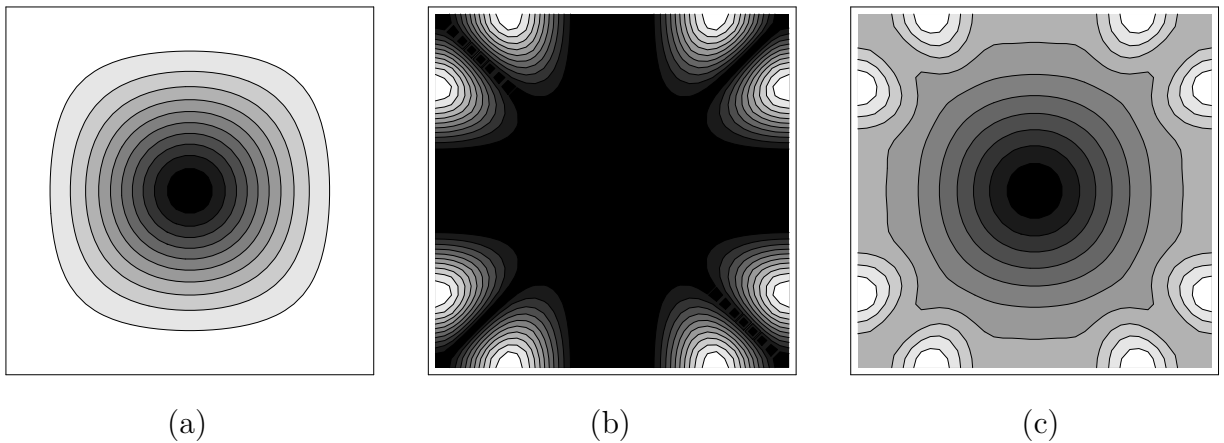


FIG. 4. A contour plot of $\Omega_{\mathbf{p}}$ vs. p_x and p_y for $p_z = 0.1$ for eqs. (a) 7.12, (b) 7.13, and (c) 7.14.

Here's an example that's degenerate in a different way:

$$[\Omega_{\mathbf{p}}^{(2)}]^2 = \left\{ (1 - \cos p_x) (\cos p_y - \cos p_z)^2 \right\} \times \{ \text{cyclic permutations} \} . \quad (7.13)$$

This example has been constructed to give $\Omega_{\mathbf{p}} = 0$ along all the planes of symmetry, and a fixed p_z slice is shown in fig. 4b. This example by itself doesn't have the right $\mathbf{p} \rightarrow 0$ behavior for the continuum theory, but we can now obtain an interesting non-degenerate example by an appropriate superposition of the two degenerate ones. For example, a p_z slice of

$$\Omega_{\mathbf{p}}^2 = [\Omega_{\mathbf{p}}^{(1)}]^2 + 5 [\Omega_{\mathbf{p}}^{(2)}]^2 \quad (7.14)$$

is plotted in fig. 4c.

VIII. THE PLASMA FREQUENCY AND DEBYE MASS

Since all the machinery was put in place in section III A, it's interesting to look at some other quantities, characteristic of classical thermal gauge theories, that are not as directly related to the topological transition rate as the damping coefficient γ . In this section, I shall examine the plasma frequency and Debye screening length at leading order in weak coupling.

The plasma frequency m_{pl} is the frequency of small-amplitude, propagating, colored waves in the long wavelength limit.¹⁸ (In quantum theories, it is also known as the plasmon mass.) It can be extracted from the general hard-loop equation (3.9) by linearizing in A^μ and taking the $\mathbf{k} \rightarrow 0$ limit for fixed ω . It's convenient to work in a covariant gauge, where this limit gives

$$\partial_\mu \partial^\mu A^i = -2C_A g^2 \int_{\mathbf{p}} \frac{dn_0}{d\Omega} v^i v^j A^j . \quad (8.1)$$

¹⁸ This concept certainly makes sense perturbatively. It is not clear (to me at least) whether there is a precise, useful, gauge-invariant, non-perturbative definition of the plasma frequency in non-Abelian gauge theory.

If the underlying theory has at least cubic symmetry, this can be rewritten as

$$\partial_\mu \partial^\mu A^i = m_{\text{pl}}^2 A^i, \quad (8.2)$$

where

$$m_{\text{pl}}^2 = -\frac{2}{3} C_A g^2 \int_{\mathbf{p}} \frac{dn_0}{d\Omega} |\mathbf{v}|^2. \quad (8.3)$$

For a classical theory, this is

$$m_{\text{pl}}^2 = \frac{2}{3} C_A g^2 T \int_{\mathbf{p}} \frac{|\mathbf{v}|^2}{\Omega^2}. \quad (8.4)$$

For the Kogut-Susskind Hamiltonian on a simple cubic lattice, the dispersion relationship (5.1) gives

$$m_{\text{pl}}^2 = 0.08606 C_A g^2 \quad (8.5)$$

in lattice units.

The plasma frequency is in fact related to the physics of topological transitions. When the system crosses the potential energy barrier for such transitions, it oscillates many times back and forth across the barrier for each net transition [6]. These oscillations are small amplitude, and their oscillation frequency is the plasma frequency. For comparison, a typical SU(2) simulation by Ambjørn and Krasnitz [4] has couplings given by $\beta_L \equiv 4/g^2 = 12$, for which (8.5) predicts a plasma oscillation period of $2\pi/m_{\text{pl}} = 26.2$. Their simulation has time steps of 0.05 in lattice units.

Debye screening is the screening of static electric fields in a plasma. It can be seen from the small-amplitude, zero frequency behavior of (3.9), which gives

$$\nabla^2 A^0 = m_{\text{d}}^2 A^0, \quad (8.6)$$

where

$$m_{\text{d}}^2 = -2C_A g^2 \int_p \frac{dn_0}{d\Omega}. \quad (8.7)$$

For a classical theory,

$$m_{\text{d}}^2 = 2C_{\text{A}}g^2T \int_p \frac{1}{\Omega_{\mathbf{p}}^2}. \quad (8.8)$$

For the Kogut-Susskind Hamiltonian on a simple cubic lattice, this gives

$$m_{\text{d}}^2 = 0.50546 C_{\text{A}}g^2 \quad (8.9)$$

in lattice units. In fact, there is an analytic result [24]¹⁹ for the integral, and (8.9) is more precisely

$$m_{\text{d}}^2 = \frac{4}{\pi^2} (18 + 12\sqrt{2} - 10\sqrt{3} - 7\sqrt{6}) \left[K\left((2 - \sqrt{3})^2(\sqrt{3} - \sqrt{2})^2\right) \right]^2 C_{\text{A}}g^2, \quad (8.10)$$

where $K(z)$ is the complete elliptic integral of the first kind.

In the weak coupling limit, the inverse screening distance $1/m_{\text{d}}$ should be large compared to the lattice spacing. For comparison, the weakest coupling simulations in ref. [4] have $\beta_{\text{L}} = 14$, for which (8.9) gives $1/m_{\text{d}} = 1.86$ lattice spacings. So there is one physical quantity, at least, for which these simulations are only marginally in the weak-coupling limit. The implications for measuring the weak-coupling behavior of the topological transition rate are unclear.

IX. CONCLUSION

In this paper, I have presented a procedure for extracting the weak-coupling limit of the real topological transition rate from rates that could be measured in simulations. The concerns about rotational invariance originally raised by Bodeker *et al.* [7] are crucial, and a precise measurement of the rate requires a search for an effectively rotational-invariant lattice Hamiltonian. Unlike the rotational improvements familiar to Euclidean studies, simply improving the rotational invariance of higher and higher derivative terms in the small

¹⁹ $\int_p \Omega_{\mathbf{p}}^{-2}$ is $\Sigma/4\pi$ where Σ is given by eq. (A.5) of ref. [24], except that equation has a typographic error: the elliptic function K should be squared [25].

momentum limit is not enough: one must also introduce a UV cut-off distance Λ^{-1} that is large compared to the lattice spacing, as discussed in section VI.

There remain several interesting problems. One is to explicitly construct the improved Hamiltonian of section VI. Another is to survey other, simpler Hamiltonians (which would not require numerical extraction of the $a\Lambda \rightarrow 0$ limit) to find one with relatively small anisotropy as measured by $\sigma_\gamma/\bar{\gamma}$. It would also be interesting to find pure gauge theories that avoid logarithmic spikes, like the scalar QED theories discussed in sec. VII B. And, of course, there is the ongoing numerical problem of actually extracting lattice topological transition rates in the first place and verifying that they scale as g_{lat}^{10} at sufficiently small coupling.

In this paper, I have focused on extracting the real topological rate from lattice simulations where the only degrees of freedom are standard gauge link variables. An interesting alternative suggested by Hu and Müller [8] is to instead introduce additional particle degrees of freedom that are described by continuum positions $\mathbf{x}(t)$ and classical non-Abelian charges and which interact with the lattice fields. The purpose of these particles is to mimic the hard degrees of freedom of the real quantum theory and induce, in the lattice theory, the correct long-distance physics of the real theory. I would just like to point out that any proposal of this type will require very careful attention to orders of limits, because there are in fact *two* contributions to the effective long-distance theory: that of the new particles, and that of the short-distance modes of the lattice gauge fields. The latter gets large as the lattice spacing is made small and will be anisotropic. So two non-commuting limits are required of any such scheme: the limit of small lattice spacing, and a limit where the coupling to the additional particles is somehow made large so that their contribution to long-distance physics dominates.

I am particularly indebted to Dam Son for explaining to me Blaizot and Iancu's formulation of hard thermal loops and for helping me understand how to generalize it. I also thank Steve Sharpe, Rajamani Narayan, Greg Moore, Larry McLerran, Misha Shaposhnikov, and

especially Larry Yaffe for a variety of useful conversations. This work was supported by the U.S. Department of Energy, grant DE-FG03-96ER40956.

APPENDIX A: DIAGRAMMATIC DERIVATION OF γ^{ij}

In this appendix, I will verify the formula (3.13) for $\gamma^{ij}(\mathbf{k})$ —and in particular its interpretation of \mathbf{v} as the group velocity—by applying diagrammatic methods in a wide class of theories. Specifically, I will discuss the calculation of the imaginary part $\text{Im } \Pi$ of the gauge boson self-energy starting from one-loop Euclidean diagrams of the form of fig. 5a, where the line in the loop represents hard excitations, be they gauge particles, scalars, or whatever. (Diagrams of the form of fig. 5b will not give a contribution to $\text{Im } \Pi$ because they cannot be cut.) I will assume that tree-level propagators of the theory are of the form $(p_0^2 - \Omega_{\mathbf{p}}^2)^{-1}$. Color indices, which are just responsible for the overall factor of C_A in the final result (3.13) for γ , will be ignored. My first assertion is that the thermal contribution to $\text{Im } \Pi^{ij}$ is

$$\text{Im } \Pi^{ij}(\omega, \mathbf{k}) = -\frac{A_-^{ij}(\omega, \mathbf{k})}{n_{\omega}^{\text{B}}} \quad (\text{A1})$$

where n^{B} is the distribution function for bosons;

$$A_-^{ij}(\omega, \mathbf{k}) = \sum_{ab} \int_p \frac{n_{\mathbf{p}}^{(a)}}{2\Omega_{\mathbf{p}}^{(a)}} \frac{(1 \pm n_{\mathbf{p}+\mathbf{k}}^{(b)})}{2\Omega_{\mathbf{p}+\mathbf{k}}^{(b)}} (\mathcal{M}_{ab}^i)^* \mathcal{M}_{ab}^j 2\pi \delta(\Omega_{\mathbf{p}}^{(a)} - \Omega_{\mathbf{p}+\mathbf{k}}^{(b)} - \omega), \quad (\text{A2})$$

is the integrated, squared amplitude for absorption of a gauge boson by the thermal bath; and $\mathcal{M}^i = \mathcal{M}^i(K, P)$ is the vertex shown in fig. 1. The sum above is over different species and polarizations a, b of the hard particles, and the capital letters K and P will henceforth stand for the “four-vectors” (ω, \mathbf{k}) and $(\Omega_{\mathbf{p}}, \mathbf{p})$. $1 \pm n_{\mathbf{p}}$ represents the final state Bose or Fermi enhancement and should be replaced by just $n_{\mathbf{p}}$ for a classical theory.

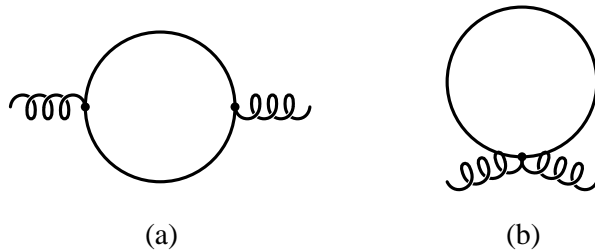


FIG. 5. Schematic contributions to the one-loop self-energy of soft gauge bosons. The loop denotes hard excitations of the theory.

(A1) is a simple consequence of the thermal optical theorem [26]. Rather than plodding through the one-loop case step by step here, I will give a quick pictorial argument for readers who are unfamiliar with it. By the contour trick for doing Euclidean finite-temperature sums, or by simply starting directly with a real-time formulation of thermal perturbation theory, the thermal contribution to the self-energy diagram of fig. 5a is given by the diagrams of fig. 6, which represent forward scattering of the soft excitation off of other excitations in the thermal bath. The imaginary part corresponds to cutting these diagrams and putting the cut line on shell. For the retarded self-energy, where ω is treated as $\omega + i\epsilon$, this cutting yields the net decay rate (actually, the rate times -2ω) of excitations: $-\text{Im } \Pi$ is the *difference* $A_- - A_+$ shown in fig. 7 of the square amplitudes A_- for destroying soft quanta and A_+ for creating them. By the principle of detailed balance (which is indeed obeyed diagrammatically), these amplitudes must satisfy

$$n_\omega A_+ = A_-(1 + n_\omega), \quad (\text{A3})$$

from which one then has

$$\text{Im } \Pi = -(A_- - A_+) = -\frac{A_-}{n_\omega}. \quad (\text{A4})$$

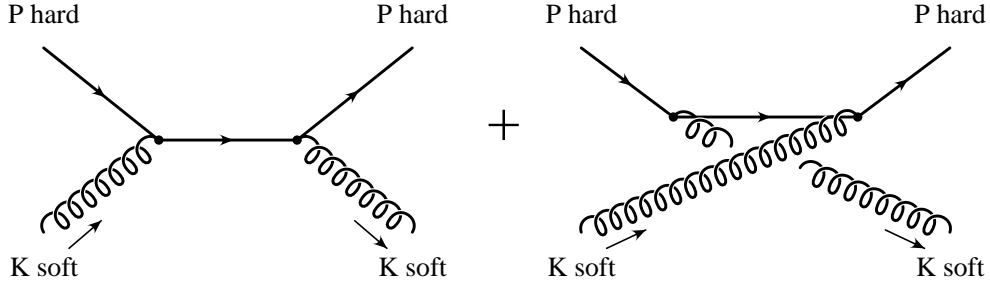


FIG. 6. A picture of the thermal part of fig. 5a as forward scattering off of particles in the thermal bath. The external hard lines are on shell.

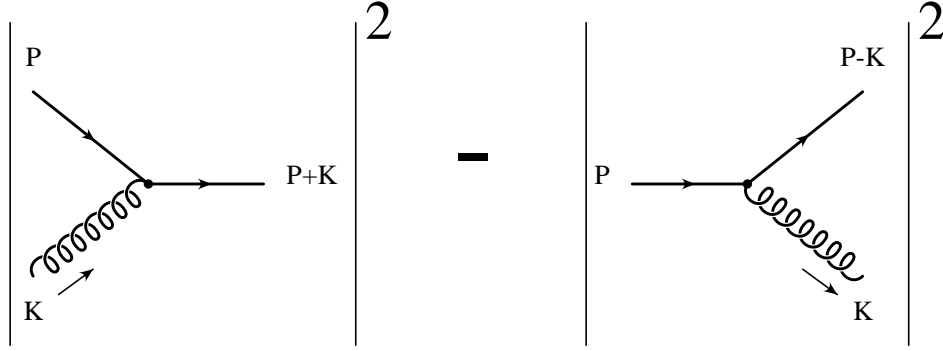


FIG. 7. A picture of $-\text{Im}\Pi$ as corresponding to the difference between absorption and emission processes of soft quanta by scattering of hard particles in the plasma.

So return to (A1). Taking the limit that both ω and \mathbf{k} are small and the limit that $\omega \ll k$ gives

$$\begin{aligned}
 \text{Im}\Pi^{ij} &\simeq -2\pi\beta\omega \sum_{\Omega^{(a)}=\Omega^{(b)}} \int_p n_{\mathbf{p}}(1 \pm n_{\mathbf{p}}) \frac{(\mathcal{M}_{ab}^i)^* \mathcal{M}_{ab}^j}{4\Omega_{\mathbf{p}}^2} \delta(\mathbf{v}_a \cdot \mathbf{k}) \\
 &= 2\pi\omega \sum_{\Omega^{(a)}=\Omega^{(b)}} \int_p \frac{dn}{d\Omega} \frac{(\mathcal{M}_{ab}^i)^* \mathcal{M}_{ab}^j}{4\Omega_{\mathbf{p}}^2} \delta(\mathbf{v}_a \cdot \mathbf{k}) \tag{A5}
 \end{aligned}$$

The sum over flavors is now restricted to pairs of flavors that have degenerate dispersion relationships. The result (3.13), or its generalization to other theories, will now follow if \mathcal{M}_{ab} can be replaced by $g\nabla(\Omega_{\mathbf{p}}^2)\delta_{ab} = 2g\Omega_{\mathbf{p}}\mathbf{v}_a\delta_{ab}$: that is, if soft magnetic gauge bosons indeed couple to group velocity. I'll argue this by surveying a few instructive examples.

As the first class of theories to check, start with a continuum scalar QED theory with a Lagrangian with scalar interactions of the form

$$\mathcal{L}_{\text{scalar}} = (\partial_t \phi_a)^* (\partial_t \phi_a) - \phi_a^* f_{ab}(\mathbf{D}) \phi_b, \quad (\text{A6})$$

where a and b are flavor indices. For the one flavor case, everything is trivial. The dispersion relationship is $\Omega_{\mathbf{p}}^2 = f(\mathbf{p})$, and the trilinear coupling with the photon is $g\phi^*\phi\mathbf{A} \cdot \nabla f$; so \mathcal{M} has the desired form.

The case of multiple flavors is slightly less trivial and is worth understanding because it is analogous to the case of multiple branches in lattice non-Abelian gauge theory. Let $U(\mathbf{p})$ be the unitary matrix that diagonalizes $f(\mathbf{p})$ in flavor space, so that $F = U^\dagger f U$ is diagonal. It's diagonal elements F_a are just the $\Omega_{\mathbf{p}}^2$ for the different branches. In this energy eigenbasis, the trilinear coupling is not in general diagonal:

$$\mathcal{M} = U^\dagger (\nabla f) U = \nabla F + U^\dagger (\nabla U) F + F (\nabla U^\dagger) U = \nabla F + [U^\dagger \nabla U, F], \quad (\text{A7})$$

so that

$$\mathcal{M}_{ab} = \nabla F_a \delta_{ab} + (U^\dagger \nabla U)_{ab} (F_b - F_a). \quad (\text{A8})$$

But the degeneracy condition on the flavor sum in (A5) eliminates the second term above, and so one obtains

$$\gamma^{ij}(\mathbf{k}) = -2\pi \sum_a g^2 \int_{\mathbf{p}} \frac{dn_0}{d\Omega} v_a^i v_a^j \delta(\mathbf{v}_a \cdot \mathbf{k}). \quad (\text{A9})$$

This is indeed the trivial generalization of (3.13) to include a sum over branches.

Now consider scalar QED on a spatial lattice, with the gradient energy given by some sum of local terms of the form

$$|\phi(\mathbf{x}) - U_{\mathbf{xy}} \phi(\mathbf{y})|^2, \quad (\text{A10})$$

where $U_{\mathbf{xy}}$ is the product of $U(1)$ link matrices along some path from \mathbf{x} to \mathbf{y} . (The canonical case would be that \mathbf{x} and \mathbf{y} are nearest neighbors and the path is the single link between them.) I am only interested in the $\phi^* A \phi$ coupling in perturbation theory and only in the limit of soft momentum for A . In this limit, $U_{\mathbf{xy}} \approx 1 + g(\mathbf{x} - \mathbf{y}) \cdot \mathbf{A}$ and the coupling is

minimal. That is, the coupling has the form (A6) in momentum space in the soft photon limit, and the previous discussion applies.

Similar considerations hold for non-Abelian lattice gauge theories. Schematically, write $A = A_{\text{soft}} + A_{\text{hard}}$ where A_{soft} are the soft-momentum modes and A_{hard} the hard momentum modes. Under *soft* gauge transformations G , we have $A_{\text{soft}} \rightarrow GA_{\text{soft}}G^{-1} - g^{-1}G\nabla G^{-1}$ and $A_{\text{hard}} \rightarrow GA_{\text{hard}}G^{-1}$. Gauge invariance under soft gauge transformations then implies that the $A_{\text{hard}}A_{\text{soft}}A_{\text{hard}}$ coupling must be minimal in the soft limit. That is, it again has the form of (A6) in the soft limit with ϕ representing A_{hard} and $\mathbf{D} = \nabla - g\mathbf{A}_{\text{soft}}^a\mathcal{T}^a$ where \mathcal{T}^a are the (anti-Hermitian) adjoint-representation generators.

As a check, it is easy to explicitly verify that the soft-hard-hard coupling of the Kogut-Susskind Hamiltonian on a simple cubic lattice indeed has $\mathcal{M}_{ab} = g\nabla(\Omega_{\mathbf{p}}^2)\delta_{ab}$, where a and b are the polarizations of the hard gluons.

APPENDIX B: NUMERICAL INTEGRALS FOR $\text{tr } \gamma$

For the sake of completeness, I will explicitly write down the two-dimensional integrals corresponding to (3.13) that I did numerically to produce figs. 2b and c.

1. Simple cubic case

$$\text{tr } \gamma(\hat{\mathbf{k}}) = \frac{1}{4\pi^2|\mathbf{k}|} C_A g^2 \int_{-\pi}^{+\pi} dp_x dp_y \sum_{p_z} \frac{|\mathbf{v}|^2}{\Omega_{\mathbf{p}}} \frac{\theta(1 - |\sin p_z|)}{|\hat{k}_z \cos p_z|}, \quad (\text{B1})$$

where the p_z sum is over two values p_z^\pm with

$$\sin p_z = -\frac{\hat{k}_x}{\hat{k}_z} \sin p_x - \frac{\hat{k}_y}{\hat{k}_z} \sin p_y, \quad (\text{B2a})$$

$$\cos p_z = \pm \sqrt{1 - \sin^2 p_z}, \quad (\text{B2b})$$

$$\sin^2\left(\frac{p_z}{2}\right) = \frac{1}{2}(1 - \cos p_z). \quad (\text{B2c})$$

$\Omega_{\mathbf{p}}$ and \mathbf{v} are given by (5.1) and (5.2).

2. FCC case

$$\begin{aligned} \text{tr } \gamma(\hat{\mathbf{k}}) = & \frac{1}{8\pi^2|\mathbf{k}|} C_A g^2 \int_{-2\pi}^{+2\pi} dp_x dp_y \sum_{\Omega_{\pm}} \sum_{p_z} \frac{|\mathbf{v}_{\pm}|^2}{\Omega_{\pm}} \frac{2\sqrt{1 - \frac{1}{16}\epsilon_{\mathbf{p}}}}{\left|B \cos\left(\frac{p_z}{2}\right) - A \sin\left(\frac{p_z}{2}\right)\right|} \\ & \times \theta(A^2 + B^2 - C^2) \theta\left(1 - \left|\sin\left(\frac{p_z}{2}\right)\right|\right), \end{aligned} \quad (\text{B3})$$

where the Ω sum is over the two dispersion relations (7.7); $\epsilon_{\mathbf{p}}$ and \mathbf{v}_{\pm} are given by (7.5) and (7.8) with $\Omega_{\mathbf{p}} = \Omega_{\pm}$; the p_z sum is over two values p_z^{\pm} with

$$\sin\left(\frac{p_z}{2}\right) = \frac{BC \pm A\sqrt{A^2 + B^2 - C^2}}{A^2 + B^2}, \quad (\text{B4a})$$

$$\cos\left(\frac{p_z}{2}\right) = \frac{AC \mp B\sqrt{A^2 + B^2 - C^2}}{A^2 + B^2}; \quad (\text{B4b})$$

and

$$A \equiv \hat{k}_x \left[\sin\left(\frac{p_y}{2}\right) + \sin\left(\frac{p_z}{2}\right) \right], \quad (\text{B5})$$

$$B \equiv \hat{k}_z \left[\cos\left(\frac{p_x}{2}\right) + \cos\left(\frac{p_y}{2}\right) \right], \quad (\text{B6})$$

$$C \equiv -\hat{k}_x \sin\left(\frac{p_x}{2}\right) \cos\left(\frac{p_y}{2}\right) - \hat{k}_y \sin\left(\frac{p_y}{2}\right) \cos\left(\frac{p_x}{2}\right). \quad (\text{B7})$$

The $\pm(\mp)$ sign in (B4) is unrelated to that in (7.7).

REFERENCES

- [1] K. Kajantie, M. Laine, K. Rummukainen, and M. Shaposhnikov, CERN report CERN-TH/96-126, hep-ph/9605288.
- [2] P. Arnold and L. McLerran, Phys. Rev. D **37**, 1020 (1988).
- [3] S. Elitzur, Phys. Rev. **D12**, 3978 (1975).
- [4] J. Ambjørn and A. Krasnitz, Phys. Lett. **B362**, 97 (1995).
- [5] D. Grigoriev and V. Rubakov, Nucl. Phys. **B299**, 671 (1988); D. Grigoriev, V. Rubakov, and M. Shaposhnikov, Nucl. Phys. **B308**, 885 (1988).
- [6] P. Arnold, D. Son, and L. Yaffe, U. of Washington preprint UW/PT-96-19, hep-ph/9609481.
- [7] D. Bodeker, L. McLerran, and A. Smilga, Phys. Rev. **D52**, 4675 (1995).
- [8] C. Hu and B. Müller, Duke U. preprint DUKE-TH-96-133, hep-ph/9611292.
- [9] T. Schäfer and E. Shuryak, hep-ph/9610451.
- [10] J. Vink, Phys. Lett. **B212**, 483 (1988).
- [11] W.-H. Tang and J. Smit, ITFA-96-11, hep-lat/9605016.
- [12] G. Moore and N. Turok, Cambridge Univ. preprint DAMPT 96-77, hep-ph/9608350.
- [13] P. Huet and D. Son, U. of Washington preprint UW/PT 96-20, hep-ph/9610259.
- [14] H. Weldon, Phys. Rev. D **26**, 1394 (1982); U. Heinz, Ann. Phys. (N.Y.) **161**, 48 (1985); **168**, 148 (1986).
- [15] M. Carrington, Phys. Rev. D **45**, 2933 (1992).
- [16] E. Braaten and R. Pisarski, Phys. Rev. D **45**, 1827 (1992); Nucl. Phys. **B337**, 569 (1990).

- [17] J.-P. Blaizot and E. Iancu, Nucl. Phys. **B390**, 589 (1993).
- [18] J.-P. Blaizot and E. Iancu, Nucl. Phys. **B417**, 608 (1994).
- [19] P. Kelly, Q. Liu, C. Lucchesi, and C. Manuel, Phys. Rev. Lett. **72**, 3461 (1994); Phys. Rev. D **50**, 4209 (1994).
- [20] G. Moore, Nucl. Phys. **B480**, 689 (1996).
- [21] H. Neuberger, Phys. Lett. **199B**, 536 (1986).
- [22] W. Celmaster and K. Moriarty, Phys. Rev. D **36**, 1947 (1987); W. Celmaster, E. Kovács, F. Green, and R. Gupta, Phys. Rev. D **33**, 3022 (1986); and reference therein.
- [23] P. Gosar, Nuovo Cim. **65B**, 329 (1981).
- [24] K. Farakos, K. Kajantie, K. Rummukainen, M. Shaposhnikov, Nucl. Phys. **B442**, 317 (1995).
- [25] M. Shaposhnikov, private communication.
- [26] R. Kobes, Phys. Rev. D **43**, 1269 (1991) and references therein.

This figure "figimpib2.gif" is available in "gif" format from:

<http://arxiv.org/ps/hep-ph/9701393v1>

This figure "figimpic2.gif" is available in "gif" format from:

<http://arxiv.org/ps/hep-ph/9701393v1>